

Update of Correlation Analysis between Active Galactic Nuclei and Ultra-High Energy Cosmic Rays

Hang Bae Kim* and Jihyun Kim†

*Department of Physics and The Research Institute of Natural Science,
Hanyang University, Seoul 133-791, Korea*

We update the previous analysis of correlation between ultra-high energy cosmic rays (UHECR) and active galactic nuclei (AGN), using 69 UHECR events with energy $E \geq 55$ EeV released in 2010 by Pierre Auger observatory and 862 AGN within the distance $d \leq 100$ Mpc listed in the 13th edition of Véron-Cetty and Véron AGN catalog. To make the test hypothesis definite, we use the simple AGN source model in which UHECR are originated both from AGN, with the fraction f_A , and from the isotropic background. We treat all AGN as equal sources of UHECR, and introduce the smearing angle θ_s to incorporate the effects of intervening magnetic fields. We compare the arrival direction distributions observed by PAO and expected from the model by the correlational angular distance distribution (CADD) and the flux-exposure value distribution (FEVD) methods. Both CADD and FEVD methods rule out the AGN dominance model with a small smearing angle ($f_A \gtrsim 0.7$ and $\theta_s \lesssim 6^\circ$). Concerning the isotropy, CADD shows that the distribution of PAO data is marginally consistent with isotropy. The best fit model lies around the AGN fraction $f_A = 0.4$ and the moderate smearing angle $\theta_s = 10^\circ$. For the fiducial value $f_A = 0.7$, the best probability of CADD was obtained at a rather large smearing angle $\theta_s = 46^\circ$. Our results imply that for the whole AGN to be viable sources of UHECR, either an appreciable amount of additional isotropic background or the large smearing effect is required. Thus, we try to bin the distance range of AGN to narrow down the UHECR sources and found that the AGN residing in the distance range 60 – 80 Mpc have good correlation with the updated PAO data. It is an indication that further study on the subclass of AGN as the UHECR source may be quite interesting.

PACS numbers: 98.70.Sa

Keywords: cosmic rays, active galactic nuclei, angular correlation

* hbkim@hanyang.ac.kr

† jihyunkim@hanyang.ac.kr

I. INTRODUCTION

The recent confirmation of the Greisen-Zatsepin-Kuzmin (GZK) suppression in the cosmic ray energy spectrum [1, 2] indicates that the ultra-high energy cosmic rays (UHECR) with energies above the GZK cutoff, $E_{\text{GZK}} \sim 40 \text{ EeV}$ ($1 \text{ EeV} = 10^{18} \text{ eV}$), mostly come from relatively close (within the GZK radius, $r_{\text{GZK}} \sim 100 \text{ Mpc}$) extragalactic sources. However, the identification of the UHECR sources is far from clear. Recent efforts to identify the sources are based on the belief that the intergalactic magnetic fields are not so strong that they don't alter significantly the trajectories of UHECR with these highest energy and thus the arrival directions of UHECR keep some correlations with the source distribution. An important step toward this direction is to check the correlation between the UHECR arrival directions and the large scale structures manifested in the galaxy distribution. It was studied by several groups [3–10] and the results are not quite conclusive yet. The positive result will provide the basis for the further study of correlations between the UHECR and specific classes of astrophysical objects. Another important progress toward this direction was the correlation between arrival directions of UHECR and nearby active galactic nuclei (AGN) reported by the Pierre Auger Observatory (PAO) [8]. Though further analysis with more data weakened the significance of the correlation [9, 10], it still remains as an important issue.

For the study of correlation between the arrival directions of UHECR and some astrophysical objects, we have to rely on the statistical methods. This is because the current limit of angular resolution in CR experiments and a poor understanding of the intergalactic magnetic fields make it difficult to pin down individual sources of UHECR from their arrival directions. This also seems to be unavoidable as we consider that currently the number of astrophysical objects which are candidates for UHECR sources is much larger than the number of observed UHECR events.

Statistical studies of correlation between the arrival directions of UHECR and the astrophysical objects were done in many ways [8–17]. In our previous paper [17], we developed new statistical test methods based on the previously used methods and combine them to obtain more reliable estimates of the significance of correlation. The basic idea is that we reduce the two-dimensional distribution of arrival directions to the one-dimensional probability distributions, which can be compared by using the well-known Kolmogorov-Smirnov (KS) test. We proposed a few reduced one-dimensional distributions suitable for the test of correlation between the UHECR arrival directions and the point sources of UHECR, which will be restated in detail in Sec. III. To make the statistical test more definite, we set up the simple AGN model for the UHECR sources, in which all or a fraction of UHECR above a certain energy cutoff are originated from the AGN lying within a certain distance cut. For simplicity, we assume that all selected AGN have the equal luminosity and smearing angle of UHECR. The remaining fraction is filled with the isotropic component of UHECR to account for the contribution from the sources outside of the distance cut. For this simple AGN model for UHECR sources, our test method showed that the correlation between UHECR in the PAO data released in 2007 and AGN listed in the 12th edition of Véron-Cetty and Véron (VCV) catalog is much stronger than the simple isotropic distribution of UHECR, but also that the correlation is not strong enough to support the hypothesis that UHECR are completely originated from AGN.

In this paper, we revisit this for two reasons. Firstly, there appeared the updated data sets both for UHECR and for AGN. We use the updated AGN data listed in the 13th

edition of VCV catalog [18] and the updated UHECR data reported by PAO in 2010 [10]. The 13th edition of VCV catalog published in 2010 is a compilation of all known AGN from a variety of catalogs, which contains 133,336 quasars, 1,374 BL Lac objects, and 34,231 active galaxies, making a total of 168,941. Especially, the number of objects lying within the GZK radius (~ 100 Mpc) which are used for the test of correlation with UHECR is 862, which is larger by about 200 than that of the previous version of catalog. PAO also published the updated data set in 2010. They released 69 UHECR events collected by the surface detector from 1 January 2004 to 31 December 2009. The data have energies above 55 EeV and zenith angle within 60° . The energy threshold is changed because PAO refined the reconstruction algorithms; however, the updated data includes all previous UHECR events listed in the previous paper. Secondly and more importantly, in the previous paper the significance estimation in the statistical test was done in an incorrect way, thus resulted in too strong constraints on the simple AGN model. Now, we performed the Monte-Carlo simulations to get the correct significance estimations. This results in the significant change in the conclusion concerning the isotropy of UHECR events.

This paper is organized as follows. In section II, we describe the simple AGN model for the UHECR sources and the details needed for the generation of Monte-Carlo events for the model and the statistical comparison with the observed data. In section III, we explain in detail our statistical methods for comparing two distributions of arrival directions. The results of our correlation analysis are presented in Section IV and discussion and conclusion follow in section V.

II. THE SIMPLE AGN MODEL FOR UHECR SOURCES

We examine the plausibility of the idea that AGN are the main sources of UHECR through the statistical comparison of the arrival direction distribution of observed UHECR data and that expected from the AGN source model. To make the implications and the limitations of our analysis more definite, we need to clearly state the AGN model for UHECR sources. In this section, we describe the details of the simple AGN model for UHECR sources which is adopted for the correlation test of AGN and UHECR in this paper.

For the comparison with the observations, we use the UHECR data with energies higher than a certain energy cut E_c . We take E_c to be higher than the GZK cutoff, $E_{\text{GZK}} \approx 40$ EeV. The merits of taking a higher value of energy cut E_c for UHECR data in the analysis of positional correlations of UHECR arrival directions with astrophysical objects are 1) we can minimize the effect of deflection due to the galactic and extragalactic magnetic fields; 2) we can reduce the fraction of the diffuse isotropic components. The diffuse isotropic components may come from the contributions of far distant astrophysical object. We can reduce these contributions by taking the energy cut above the GZK cutoff, restricting possible sources to be extragalactic, but within the GZK radius which is around 100 Mpc. Of course, the drawback is that we have the smaller number of data, which reduces the statistical power. So we need to make a compromise in-between. We use the UHECR data released by PAO in 2010 [10]. The released data set contains 69 UHECR with energy higher than 55 EeV. To fully use the released data, we take the energy cut $E_c = 55$ EeV.

For our analysis, we use AGN listed in the 13th edition of VCV catalog [18]. We select AGN within a certain distance cut d_c . Because we apply the energy cut to UHECR data which is higher than the GZK cutoff, most of probable sources of them are expected to lie within the GZK radius, $r_{\text{GZK}} \approx 100$ Mpc. Thus, we take d_c to be 100 Mpc (corresponding to

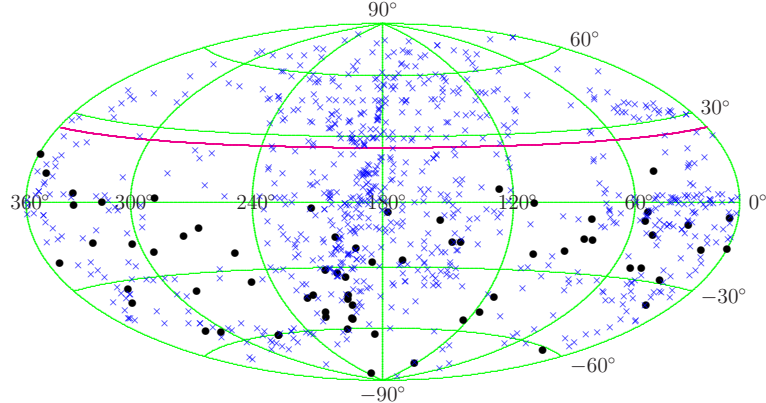


FIG. 1. Distribution of the arrival directions of UHECR, represented by black dots (\bullet), with energy $E \geq 55$ EeV reported by PAO in 2010, in the equatorial coordinates plotted using the Hammer projection. The solid red line represents the boundaries of the sky covered by PAO experiments. The blue crosses (\times) represent the locations of AGN with distance $d \leq 100$ Mpc taken from the 13th edition of VCV catalog.

the redshift $z \leq 0.024$). The original number of AGN within 100 Mpc in the VCV catalog is 865. This includes 3 AGN with zero redshift, which are problematic to be included in our analysis. Thus, we eliminate these three AGN from our AGN data set and the remaining 862 AGN will be used in our analysis. Fig. 1 shows the distributions of UHECR and AGN used in our analysis.

We consider AGN as smeared point sources of UHECR, incorporating the fact that the trajectories of UHECR can be bent by intervening magnetic fields. The smearing effect varies AGN by AGN in general. We assume that each AGN has a gaussian flux distribution with a certain angular width. Then the UHECR flux from all AGN is given by

$$F_{\text{AGN}}(\hat{\mathbf{r}}) = \sum_{j \in \text{AGN}} \frac{L_j}{4\pi d_j^2} \cdot \frac{\exp\left[-(\theta_j(\hat{\mathbf{r}})/\theta_{sj})^2\right]}{N(\theta_{sj})}, \quad (1)$$

where L_j is the UHECR luminosity, d_j is the distance, $\theta_j(\hat{\mathbf{r}}) = \cos^{-1}(\hat{\mathbf{r}} \cdot \hat{\mathbf{r}}'_j)$ is the angle between the direction $\hat{\mathbf{r}}$ and the j -th AGN, θ_{sj} is the smearing angle of the j -th AGN, and $N(\theta_{sj}) = \int d\Omega \exp[-(\theta_j(\hat{\mathbf{r}})/\theta_{sj})^2]$ is the normalization of smearing function. For small θ_s , $N(\theta_s) \approx \pi\theta_s^2$ and for large θ_s , $N(\theta_s) \approx 4\pi$. Just for simplicity, we assume that all AGN have the same UHECR luminosity, $L_j = L$, and the same smearing angle, $\theta_{sj} = \theta_s$. The value of L will be fixed by the total number of UHECR contributed by AGN. The smearing angle, θ_s , is taken to be a free parameter, while its fiducial value is taken to be 6° [3].

The UHECR with energy above the energy cut $E_c = 55$ EeV still can come from the sources lying outside the distance cut $d_c = 100$ Mpc, and we want to take it into account in the UHECR source model. We consider that a certain fraction of UHECR with energy above E_c is originated from the AGN within a distance d_c , while the remaining fraction of them is from the isotropically distributed background contributions. Thus, the expected flux at a given arrival direction $\hat{\mathbf{r}}$ is the sum of two contributions,

$$F(\hat{\mathbf{r}}) = F_{\text{AGN}}(\hat{\mathbf{r}}) + F_{\text{ISO}}. \quad (2)$$

Now we define the AGN fraction f_A to be

$$f_A = \frac{\overline{F}_{\text{AGN}}}{\overline{F}_{\text{AGN}} + F_{\text{ISO}}}, \quad (3)$$

where $\overline{F}_{\text{AGN}} = (4\pi)^{-1} \int F_{\text{AGN}}(\hat{\mathbf{r}}) d\Omega = L \cdot (4\pi)^{-2} \sum_j d_j^{-2}$ is the average AGN-contributed flux. Note that the definition of the AGN fraction is somewhat different from that defined in our previous work. There, the AGN fraction was defined to be the ratio of AGN-originated UHECR after considering the exposure of the detector array. This actual fraction of AGN contribution at a given detector is generally different from f_A because it depends on the location of the detector relative to the source distribution and on the size of the smearing angle. We found that for the PAO site considering the exposure makes the actual AGN fraction a little bit smaller than f_A . Now the UHECR flux can be written as

$$F(\hat{\mathbf{r}}) = f_A \overline{F} \frac{4\pi \sum_j d_j^{-2} \exp \left[-(\theta_j(\hat{\mathbf{r}})/\theta_s)^2 \right]}{N(\theta_s) \sum_j d_j^{-2}} + (1 - f_A) \overline{F}, \quad (4)$$

where $\overline{F} = \overline{F}_{\text{AGN}} + F_{\text{ISO}}$. Out of three parameters L , θ_s , and F_{ISO} , the AGN fraction f_A and the smearing angle θ_s are treated as the free parameters of the model, while the average flux \overline{F} is fixed by the total number of UHECR events.

If the source distribution is known, the fraction of UHECR with $E \geq E_c$ coming from the sources with $d < d_c$ can be estimated as a function of E_c and d_c by solving the cosmic ray propagation equation. For the uniform distribution of equal sources, $E_c = 55$ EeV and $d_c = 100$ Mpc, the estimated value is around $f_A \approx 0.7$ [4], and we will take this value as the fiducial value of f_A .

For the correct comparison of observed arrival directions with the expected ones, we also need to take into account the efficiency of the detector as a function of the arrival direction. It depends on the location and the characteristics of the detector array. Here we consider only the geometric efficiency which is determined by the location and the zenith angle cut of the detector array. Then the exposure function h depends only on the declination δ [19],

$$h(\delta) = \frac{1}{\pi} [\sin \alpha_m \cos \lambda \cos \delta + \alpha_m \sin \lambda \sin \delta], \quad (5)$$

where λ is the latitude of the detector array, θ_m is the zenith angle cut, and

$$\alpha_m = \begin{cases} 0, & \text{for } \xi > 1, \\ \pi, & \text{for } \xi < -1, \\ \cos^{-1} \xi, & \text{otherwise} \end{cases} \quad \text{with } \xi = \frac{\cos \theta_m - \sin \lambda \sin \delta}{\cos \lambda \cos \delta}.$$

The PAO site has the latitude $\lambda = -35.20^\circ$ and the zenith angle cut of the released data is $\theta_m = 60^\circ$.

To get the expected distribution from the simple AGN model, we rely on the simulation taking into account the exposure function. In Fig. 2, we showed the distributions of mock UHECR data for two different values of the AGN fraction, $f_A = 1.0$ and $f_A = 0.4$ with the same smearing angle $\theta_s = 6^\circ$.

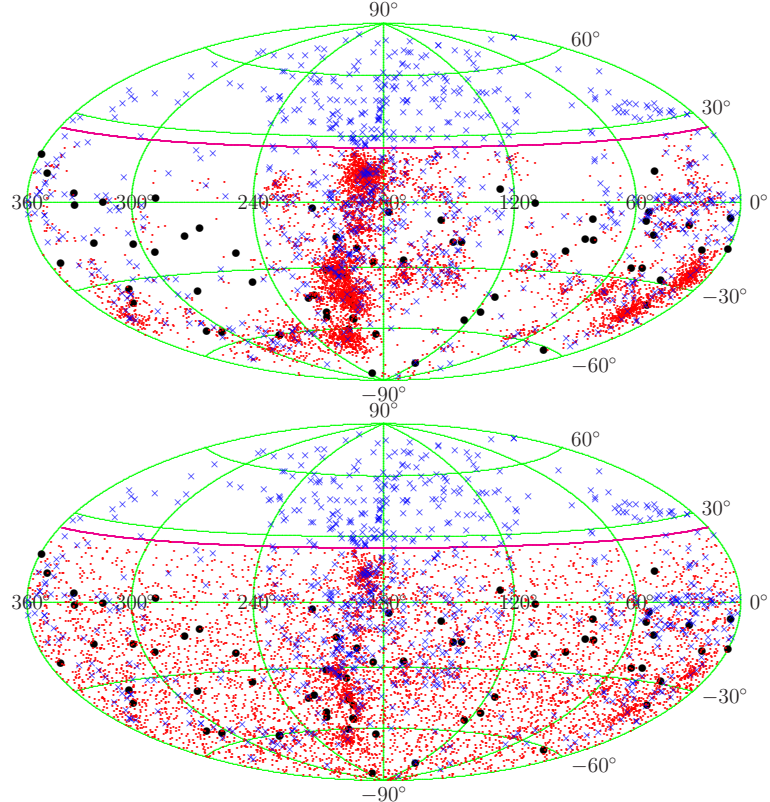


FIG. 2. Distributions of the mock UHECR arrival directions (6900 events, represented by small red dots) of PAO experiment, obtained from the simple AGN model for two different values of AGN fraction $f_A = 1$ (upper panel) and $f_A = 0.4$ (lower panel), with the same smearing angle $\theta_s = 6^\circ$. Others are same as in Fig. 1.

III. STATISTICAL COMPARISON OF TWO ARRIVAL DIRECTION DISTRIBUTIONS

We now describe our statistical methods to measure the plausibility of the UHECR source model. What we obtain through statistical analysis is the probability that the observed UHECR arrival direction distribution originates from the given UHECR source model. This is achieved by statistically quantifying how similar the observed UHECR arrival direction distribution is to the expected one from the source model. In our previous work [17], we developed comparison methods in which the two-dimensional UHECR arrival direction distributions on the sphere is reduced to one-dimensional probability distributions of some sort, so that they can be compared by using the standard one-dimensional Kolmogorov-Smirnov (KS) test. In this section we elaborate further on these methods.

As an illustration of our method, let us consider the distribution of equatorial coordinates, Right Ascension (RA) or Declination (DEC) of UHECR. Let us call them RA distribution (RAD) and DEC distribution (DECD), respectively. In this case, the reductions are simply for RAD: $\hat{\mathbf{r}}_i = (\alpha_i, \delta_i) \rightarrow \alpha_i$ and for DECD: $\hat{\mathbf{r}}_i = (\alpha_i, \delta_i) \rightarrow \delta_i$, where $\hat{\mathbf{r}}_i$ are arrival directions of UHECR. In Fig. 3, we show RAD and DECD of the PAO data and compare them with those of the isotropic distribution and of the simple AGN model with $f_A = 1.0$ and $\theta_s = 6^\circ$ described in the previous section. RAD and DECD are normalized as the probability

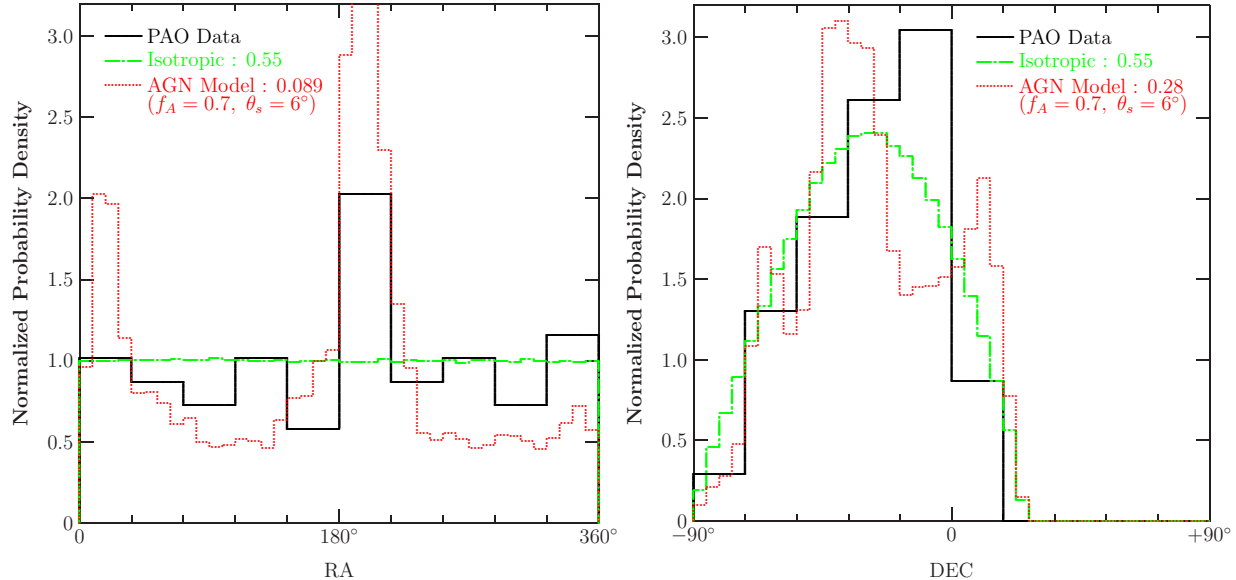


FIG. 3. RA and DEC distribution of PAO data, compared to the isotropic distribution and the simple AGN model with $f_A = 0.7$ and $\theta_s = 6^\circ$. The figure in the right hand side of the model name is the probability, obtained by the KS test, that the PAO data are yielded from the model.

distribution by dividing the count by the total number of data, so that they sum up to 1.

Now we can apply the standard KS test to measure how similar the distribution obtained from the observed data to that expected from the model. The KS test is based on the cumulative probability distribution (CPD) $S_N(x) = \int^x p(x')dx'$ and the KS statistic is the maximum difference between two CPDs $D = \max_x |S_{N_1}(x) - S_{N_2}(x)|$. Though we made binning for plotting the distribution in Fig. 3, you can easily see that the KS test does not involve binning. From the KS statistic D , the probability that the real data are obtained from the model under consideration is given approximately by [20]

$$P(D|N_e) = Q_{\text{KS}}([\sqrt{N_e} + 0.12 + 0.11/\sqrt{N_e}]D), \quad (6)$$

where $Q_{\text{KS}}(\lambda) = 2 \sum_{j=1}^{\infty} (-1)^{j-1} e^{-2j^2\lambda^2}$ and $N_e = N_1 N_2 / (N_1 + N_2)$ is the effective number of data. For RAD and DECD, the number of data in the distribution is same as the number of UHECR data. Thus, $N_1 = N_O$, the number of observed UHECR data and $N_2 = N_S$, the number of mock UHECR data. We can make the expected distribution more accurate by increasing the number of mock data N_2 from the model under consideration. In the limit $N_2 \rightarrow \infty$, the effective number of data is simply $N_e = N_O$.

The probabilities that the PAO data are obtained from the isotropic distribution and the simple AGN model with fiducial parameters ($f_A = 0.7$ and $\theta_s = 6^\circ$) are 0.55 and 0.089 by RAD, and 0.55 and 0.28 by DECD, as shown in Fig. 3. Both RAD and DECD indicate that the PAO data are consistent with isotropy, while RAD reveals that the simple AGN model with fiducial parameters is slightly disfavored.

The reduction from the two-dimensional distribution to the one-dimensional distribution implies the loss of information in the obtained data anyway. However, it is easy and conceptually transparent to compare and sometimes a good choice of reduction method can catch what causes the discrepancy between the observed data and the model prediction. RAD or DECD may be good for checking isotropy, but may not be suitable for the study of

correlation between the UHECR arrival directions and the directions of astrophysical point sources such as AGN. We can devise the reduced distributions which are more sensitive to the correlation between the sources and UHECR. In the previous paper, we introduced three methods: AADD, CADD, and FEVD. Now we focus on CADD and FEVD described below, which deal with the correlation between AGN and UHECR directly and thus are more relevant in correlation analysis.

a. Correlational Angular Distance Distribution (CADD) This is the distribution of the angular distances of all pairs UHECR arrival directions and the point source directions:

$$\text{CADD} : \left\{ \cos \theta_{ij'} \equiv \hat{\mathbf{r}}_i \cdot \hat{\mathbf{r}}'_j \mid i = 1, \dots, N; j = 1, \dots, M \right\}, \quad (7)$$

where $\hat{\mathbf{r}}_i$ are the UHECR arrival directions, $\hat{\mathbf{r}}'_j$ are the point source directions, and N and M are their total numbers, respectively. In Fig. 4, we show the concept of CADD schematically. This is also an improvement of previously adopted methods [8, 9, 13, 21] and most useful when we consider the set of point sources for UHECR. The number of data in CADD obtained from N UHECR data is $N_{\text{CADD}} = NM$. This means that the data in CADD are not all independently sampled, and the probability formula (6) which assumes the independent sampling of data cannot be used. Therefore, the probability has to be directly inferred for the source model in hand through the Monte-Carlo simulations. For this purpose, we first form a reference set consisting of a huge number of UHECR events generated from the source model. Then, we generate the mock set consisting of the same number of UHECR events as the observed data from the model and calculate the KS statistic D_{KS} between the reference set and the mock set. Then, we repeat the generation of the mock set enough times to get the probability distribution of D_{KS} . In this way, we infer the significance of $D_{\text{KS,observed}}$ between the reference set and the observed data.

b. Flux Exposure Value Distribution (FEVD) At a given arrival direction, the expected flux value is the product of the UHECR flux expected from the UHECR source model and the exposure function of the detector at that direction. FEVD is the distribution of expected flux values at UHECR arrival directions:

$$\text{FEVD} : \left\{ F_i \equiv F(\hat{\mathbf{r}}_i)h(\hat{\mathbf{r}}_i) \mid i = 1, \dots, N \right\}, \quad (8)$$

where $\hat{\mathbf{r}}_i$ are the UHECR arrival directions, N is the total numbers of UHECR, $F(\hat{\mathbf{r}}_i)$ and $h(\hat{\mathbf{r}}_i)$ are the UHECR flux and the exposure function, respectively. In Fig. 5, we show the concept of FEVD schematically. It was proposed by Koers and Tinyakov [4] to test the correlation between the galaxy distribution and the UHECR. One merit of this method is that it can be used for the continuous source distribution, as well as for the point sources. The number of data in FEVD is $N_{\text{FEVD}} = N$. Thus, the probability formula (6) can be directly used. We confirmed this fact through the Monte-Carlo simulation done in the same way as in the CADD case.

IV. CORRELATION ANALYSIS

In our previous work [17], we analyzed the correlation between the PAO data released in 2007 and the AGN listed in the 12th edition of VCV catalog. In this paper, we update the analysis using the PAO data released in 2010 and the 13th edition of VCV catalog. For moderate numbers of data, the suitable methods for the analysis of correlation between the arrival directions of UHECR and the locations of point sources such as AGN are CADD and

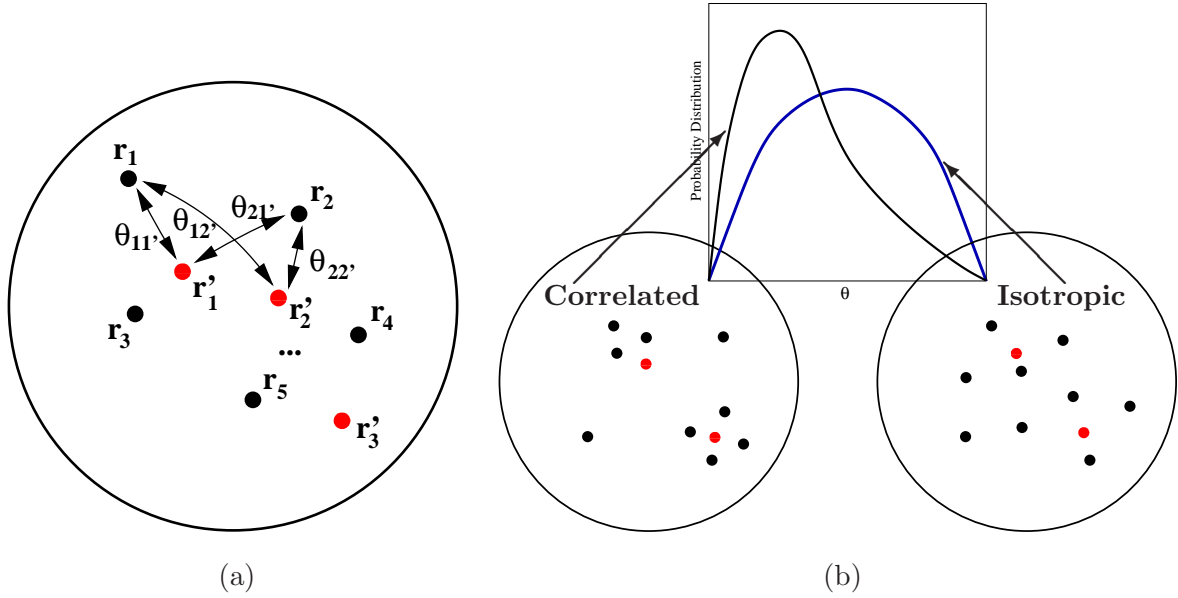


FIG. 4. Illustrations showing the basic idea of CADD and its comparison. (a) CADD is the probability distribution of all angular distances between the reference (point source) directions (red dots) and the UHECR arrival directions (black dots). (b) When the observed UHECR events are more clustered around the reference directions than, say, those of the isotropic distribution, the observed CADD has larger probability density at small angles than that expected from the isotropic distribution.

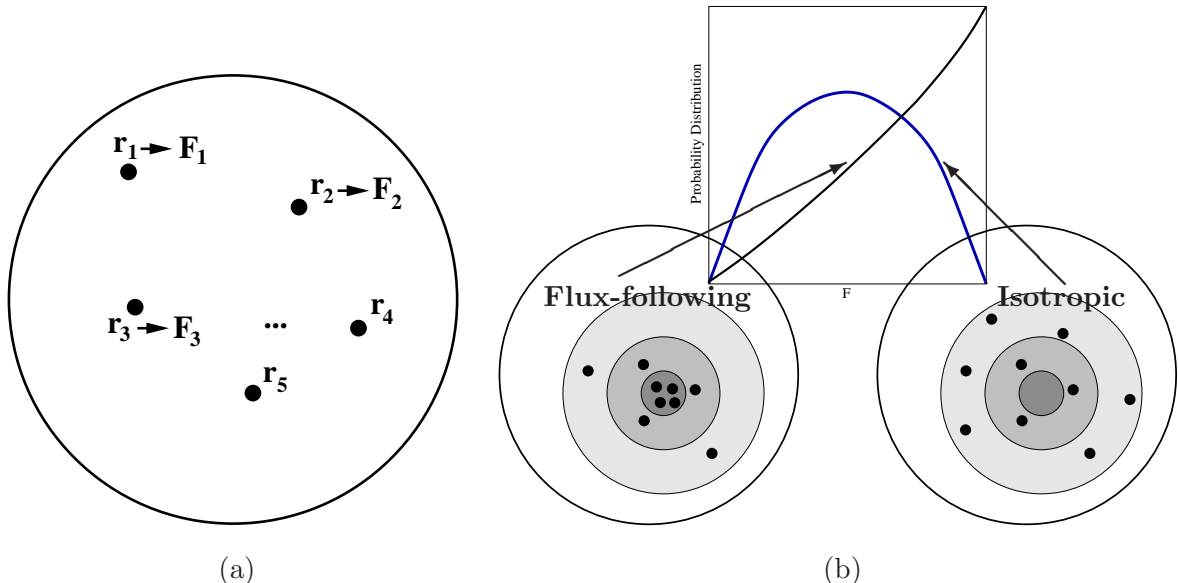


FIG. 5. Illustrations showing the basic idea of FEVD and its comparison. (a) FEVD is the probability distribution of the flux times exposure values at the UHECR arrival directions (black dots). (b) When the observed UHECR follows the flux predicted by the model more faithfully than, say, that of the isotropic distribution, the observed FEVD has larger probability density at high flux values than that expected from the isotropic distribution.

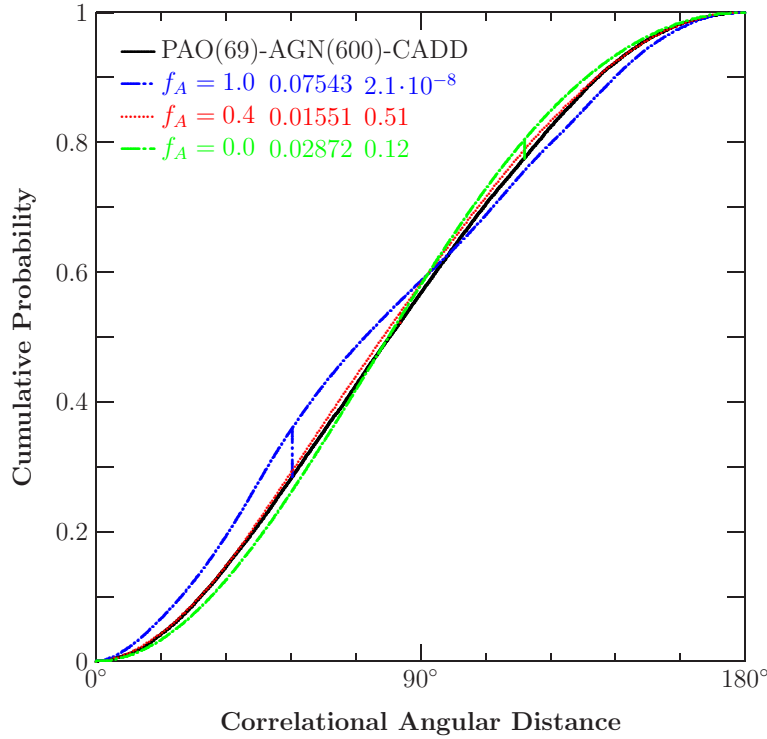


FIG. 6. The cumulative probability distributions of CADD of AGN and UHECR. The solid black is for the PAO data, the dashed green line for the isotropic distribution, the dashed blue line and the dotted red line for the simple AGN model with the smearing angle $\theta_s = 6^\circ$ and the AGN fraction $f_A = 1$ and $f_A = 0.4$, respectively. The vertical bars show the positions and sizes of the KS statistic D . The numbers in two right columns in the legend are the value of KS statistic and the probability that the distribution of PAO data is obtained from the model specified.

FEVD. Therefore, we use both CADD and FEVD to cross-check and compare the results. We also emphasize that we correct the probability calculation for CADD by using the values directly inferred through the Monte-Carlo simulations.

To get the expected distribution from the simple AGN model, we also rely on the simulation. Because we use the probability distributions for comparison, we can obtain more accurate expected distribution by increasing the number of mock UHECR data from the model. For the reason of practical computation, we use $N_S = 10^5$ which give the accuracy sufficient for our purpose within reasonable computation time.

To understand how the discrepancy between the distribution obtained from the data and that from the model occurs, it is helpful to examine the cumulative probability distribution (CPD) directly and check the position where the KS statistic is obtained. In Fig. 6, we show CPD of CADD for the PAO data and for three cases of our interest, the simple AGN model with $f_A = 0$ (completely isotropic distribution), $f_A = 1$ and $\theta_s = 6^\circ$ (complete AGN origination with a small smearing angle), and $f_A = 0.4$ and $\theta_s = 6^\circ$ (the best fit model for a smearing angle $\theta_s = 6$). We note that the stronger the correlation between UHECR and AGN is, the more UHECR lie at small angular distances from AGN, resulting in steeper rise of CPD at small angles. Thus, the small angle region of CPD in Fig. 6 reveals that the PAO data have stronger correlation with AGN than the completely isotropic distribution, but the correlation is not strong enough to be consistent with the case of complete AGN

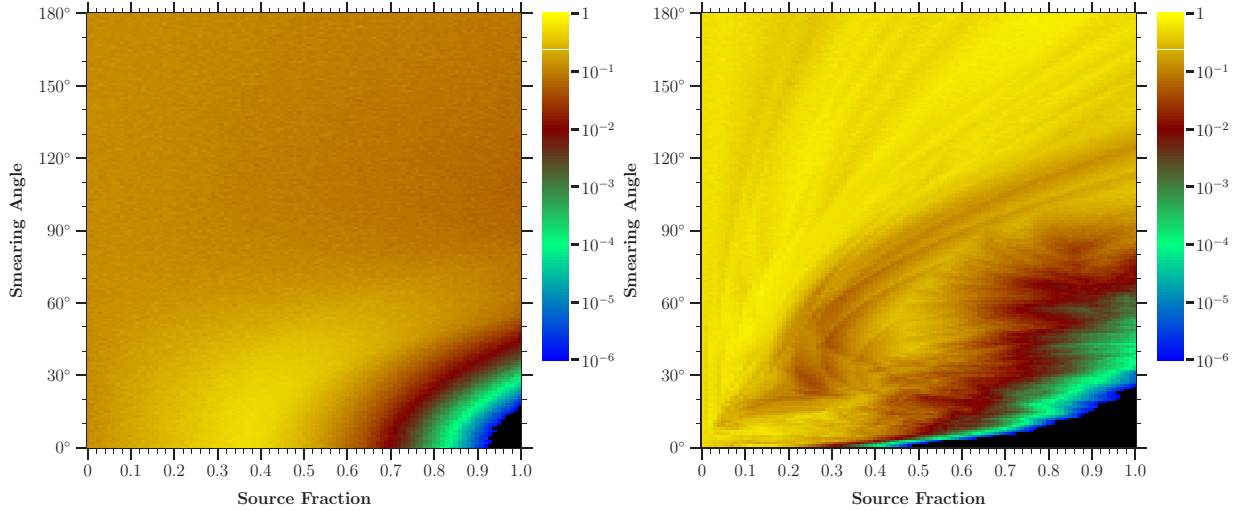


FIG. 7. AGN fraction (f_A) and smearing angle (θ_s) dependence of probabilities by CADD (left panel) and FEVD (right panel) methods for the PAO data.

origination with a small smearing angle ($\theta_s = 6^\circ$). The probabilities given by the CADD KS test indicate that the PAO data are marginally consistent with the isotropy ($P = 0.12$) but rule out the complete AGN origination with a small smearing angle ($P = 2.1 \times 10^{-8}$).

Because CPD of CADD shows that the observed PAO distribution lies between the isotropic distribution and complete AGN origination with a small smearing angle, we expect that decreasing the AGN fraction f_A (that is, adding more isotropic component) or increasing the smearing angle θ_s may improve the probability. In Fig. 7, we show f_A and θ_s dependence of probabilities by CADD and FEVD methods for the PAO data. Both CADD and FEVD methods rule out AGN dominance with small smearing angles ($f_A \gtrsim 0.7$ and $\theta_s \lesssim 6^\circ$, the lower right corner of the plot). FEVD gives stronger constraint for small smearing angles. It strongly disfavors AGN dominance even for moderately large smearing angles. For AGN dominance ($f_A \gtrsim 0.7$) to be compatible with the PAO data, the rather large smearing angle ($\theta_s \gtrsim 30^\circ$) is required. The PAO data are found to be marginally consistent with the isotropy by both CADD and FEVD methods, even though the complete isotropy is not the best fit to the PAO data by both methods.

Now, let us examine the results for the fiducial values of two parameters. In Fig. 8, we plot the AGN fraction (f_A) dependence of probability for the fiducial value of smearing angle $\theta_s = 6^\circ$. The probability by CADD reaches the maximum at $f_A = 0.37$, that by FEVD at $f_A = 0.16$. For this small value of smearing angle, FEVD gives stronger constraints than CADD and the consistency with the PAO data requires low AGN fraction ($f_A \lesssim 0.4$) and large isotropic background. Compared to the result for 2007 PAO data, the best fit value of f_A is reduced by 0.1. In Fig. 9, we plot the smearing angle (θ_s) dependence of probability, for the fiducial value of AGN fraction $f_A = 0.7$. For the PAO data to be consistent with the simple AGN model for this fixed value of the AGN fraction, the rather large smearing angle is required.

So far, our hypothesis assumed that all AGN listed in the catalog are equal sources of UHECR with $E \geq E_c$. One trouble we face concerning this fact is that the number of available UHECR data is smaller than the number of AGN. Thus, all AGN cannot be the actual sources of UHECR we consider. We took the view that the UHECR luminosity of

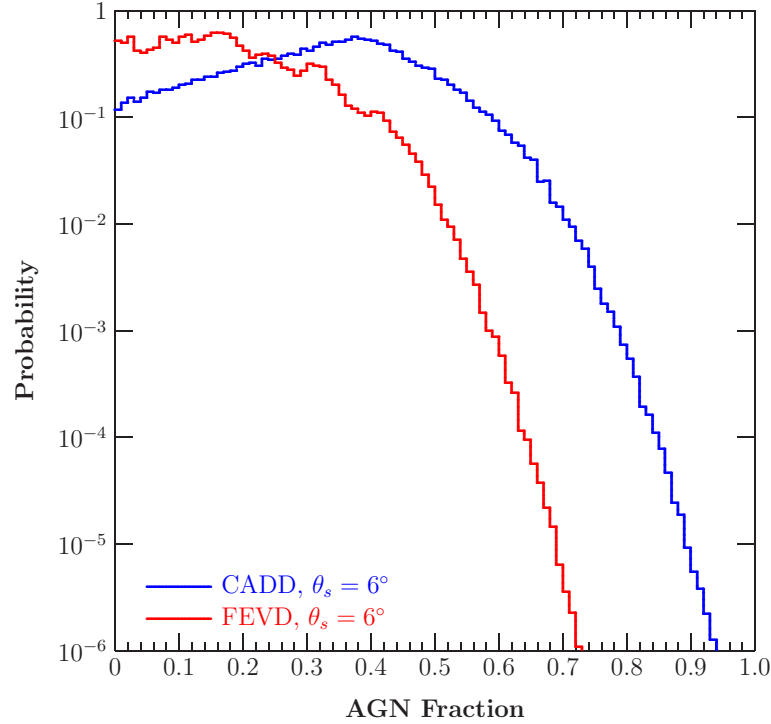


FIG. 8. AGN fraction (f_A) dependence of probabilities at a smearing angle $\theta_s = 6^\circ$ by CADD and FEVD methods.

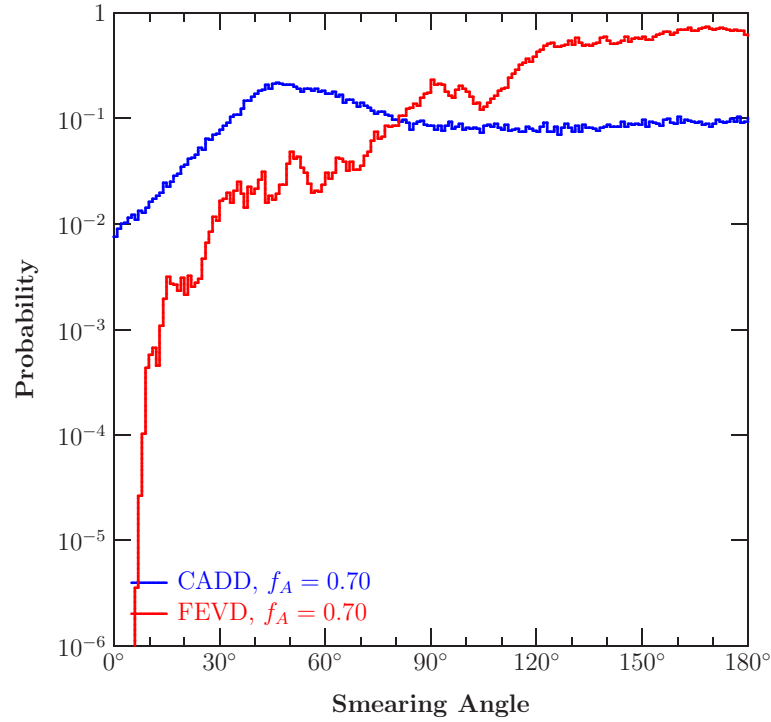


FIG. 9. Smearing-angle (θ_s) dependence of probabilities at an AGN fraction $f_A = 0.7$ by CADD and FEVD methods.

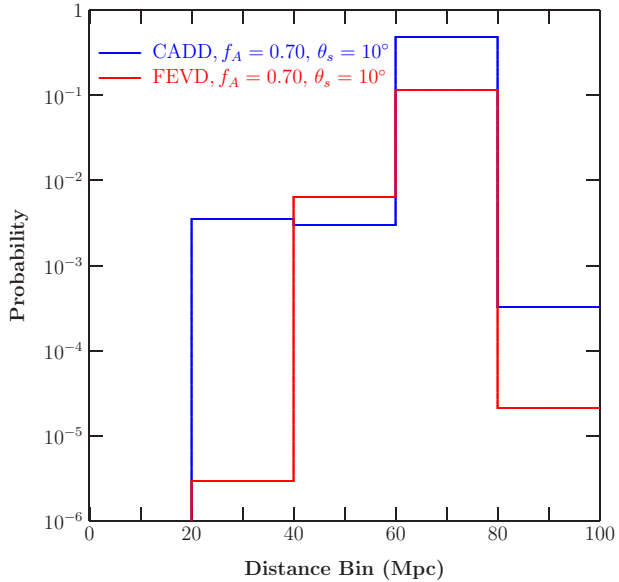


FIG. 10. Probabilities for the PAO data from the simple AGN model with AGN in the distance range of 20 Mpc bins. For the AGN fraction, the fiducial value $f_A = 0.7$ is used and for the smearing angle, the moderate value $\theta_s = 10^\circ$ is used.

AGN is small and the randomly chosen subset of AGN is responsible for observed UHECR. The other plausible possibility is that a certain subset of listed AGN is the genuine source of UHECR and the others are not. To make this hypothesis more concrete, we need to further classify AGN in some way and narrow down the source candidates among them. Toward this purpose, some people have tried the idea that the UHECR comes from AGN accompanied by the strong radiation in X-ray or γ -ray range [10, 22–28].

In our previous analysis, we tried the simple geometrical classification based on distance binning and this leaded to the rather interesting result that AGN residing in the distance range $40 - 80$ Mpc shows striking correlation with the PAO UHECR data. Thus, we perform the same analysis again. Fig. 10 shows that the correlation probabilities between PAO UHECR data and the simulation data which is obtained by assuming that the AGN residing in the each distance range are responsible for the UHECR. In this case, we set the AGN fraction $f_A = 0.7$ and smearing angle $\theta_s = 10^\circ$. The addition of new data weakens the correlation; however, CADD and FEVD have good correlation probabilities in the distance range $60 - 80$ Mpc. We can see the similar distributions between PAO UHECR data distribution and AGN in the distance range $60 - 80$ Mpc visually in Fig. 11. The analogous result was reported by Ryu et al. [29]. They measured the separation angles S between UHECR of the 2007 PAO data and their nearest AGN in the 12th edition of VCV catalog, then plotted S versus the distance of the correlated AGN. Rather independently of S , the correlated AGN are concentrated in $40 - 60$ Mpc distance range (See Fig. 5 in [29].). This is consistent with the above result. We do not have a reasonable explanation for this correlation yet. However, this correlation can possibly be interpreted as the imprint of the large scale structure of the universe or as an indication that a certain subclass of AGN is the genuine source of UHECR.

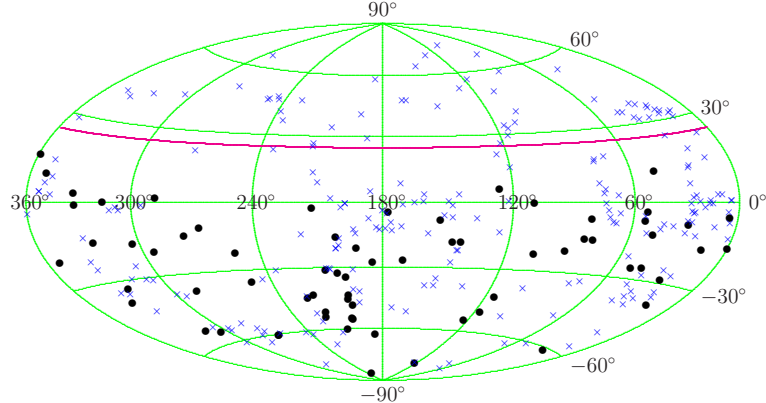


FIG. 11. Distributions of AGN in the $60 - 80$ Mpc distance range and the arrival directions of UHECR with $E \geq 55$ EeV observed by PAO.

V. DISCUSSION AND CONCLUSION

The PAO firstly reported the correlation between AGN and UHECR in 2007 [8, 9]. They found 20 out of 27 UHECR events with energies above 57 EeV are correlated with at least one of the 442 AGN within the distance 71 Mpc listed in the 12th edition of VCV catalog when they fixed the correlation angular distance to be $\psi = 3.2^\circ$. In the updated paper published in 2010 [10], the energy threshold was modified from 57 EeV to 55 EeV due to the energy calibration and the other parts of correlation test method remained same. They divide the 69 UHECR data with energies above 55 EeV detected from 1 January 2004 to 31 December 2009 into three periods. Using the data of Period 1, they set up the three parameters, the distance cutoff for AGN $d_c \leq 75$ Mpc, the energy threshold for UHECR 55 EeV, and the correlation angular distance $\psi = 3.1^\circ$, through the exploratory scan and minimizing the chance probability that the observed UHECR events come from the simple isotropic distribution. These parameters are applied to other data sets and the correlations between UHECR and AGN are tested. As a result, 17 out of 27 events are correlated with the AGN and the degree of correlation, which is defined to be the fraction of correlated events, $p_{\text{data}} = 0.63$ is obtained by using the data presented in 2007 paper (Period 1 + Period 2). When the updated data are used, 29 out of 69 events are located within the correlation angular distance, therefore the degree of correlation is reduced to $p_{\text{data}} = 0.42$. For more strict examination, the data used in the exploratory scan need to be excluded. When only the data detected during Period 2 and Period 3 are used, 21 out of 55 events are correlated and the degree of correlation is reduced further to $p_{\text{data}} = 0.38$. If the isotropic distribution is assumed, the number of expected correlated events is 11.6 and the probability of finding such a correlation by chance is $P = 0.003$. (See the Table 1 in [10].) This means that the updated PAO data says that the distribution of UHECR is neither completely isotropic nor correlated with AGN very strongly.

However, as we noted in the previous paper [17], PAO's method is not sufficient to prove the correlation between AGN and UHECR. For the correlation test, our test methods are more direct and informative. The change in the results obtained from our test methods for the 2007 PAO data and for the updated data in 2010 seem to be consistent with that of PAO's method. Let us look into the details in terms of the best probability. The previous results of AGN fraction scan (the smearing angle $\theta_s = 6^\circ$) had the best probability at $f_A = 0.45$

in the case of CADD and at $f_A = 0.42$ in the case of FEVD; however, when the updated data are used, CADD has the maximum at $f_A = 0.37$ and FEVD has $f_A = 0.16$ (See the Fig. 8.). In the case of smearing angle scan, (the AGN fraction is fixed as $f_A = 0.7$) the best smearing angle which have the maximum probability shifts from $\theta_s = 36^\circ$ to $\theta_s = 46^\circ$ for the CADD and from $\theta_s = 45^\circ$ to $\theta_s = 168^\circ$ for the FEVD (See the Fig. 9.). This means that the AGN model needs more isotropic component to describe the UHECR distribution, and this is consistent with the results of PAO. We can interpret that the updated data are more isotropic than the previous data.

We used the 13th edition of VCV catalog for the AGN information. However, the VCV catalog is an incomplete one in the sense that it is not a catalog obtained from a single observational mission and it does not cover the full sky completely. Therefore, it has a certain limitation to use the VCV catalog for the correlation test. PAO also mentioned this point and they considered the incompleteness of VCV catalog in the galactic plane region. There are 9 UHECR events within $\pm 10^\circ$ from the galactic plane. When they exclude these data to calibrate the incompleteness of the galactic plane region, the correlation is increased from $p_{\text{data}} = 0.38$ to $p_{\text{data}} = 0.46$, i.e. 21 out of 46 are within the correlation angular window. It is hard to say that the results are statistically significant. When we apply this approach to CADD, the best value of the AGN fraction is increased slightly to $f_A = 0.41$, while the best value of the smearing angle, $\theta_s = 45^\circ$, is similar to the result for the whole data set. We cannot see the significant effect of incompleteness in the galactic plane region at this step. Also, we cannot confirm that these results are caused by the incompleteness of catalog or by the deflection due to the strong magnetic field in galactic plane region. These possibilities need to be explored further.

In conclusion, we reexamined the correlation between UHECR and AGN using the updated data sets: for UHECR, we used 69 events with energy $E \geq 55$ EeV released in 2010 by PAO and for AGN, we used 862 AGN within the distance $d \leq 100$ Mpc listed in the 13th edition of VCV catalog. To make the test hypothesis definite, we built up the simple AGN model in which UHECR are originated both from AGN, with the fraction f_A , and from the isotropic background. We treated all AGN as equal sources of UHECR. We also introduced the smearing angle θ_s to incorporate the effects of galactic and extragalactic magnetic fields. Then we compared the arrival direction distributions observed by PAO and expected from the model by CADD and FEVD methods. These methods reduce the two-dimensional arrival direction distribution to one dimensional probability distribution which reflect the correlation between UHECR and their source candidates so that we can apply the standard KS test and calculate the chance probability that the observed distribution comes from the model.

Our results show that both CADD and FEVD methods rule out the AGN dominance model with a small smearing angle ($f_A \gtrsim 0.7$ and $\theta_s \lesssim 6^\circ$). Concerning the isotropy, CADD shows that the distribution of PAO data is marginally consistent with isotropy. The best fit model lies around the AGN fraction $f_A = 0.4$ and the moderate smearing angle $\theta_s = 10^\circ$. For the fiducial value $f_A = 0.7$, the best probability of CADD was obtained at a rather large smearing angle $\theta_s = 46^\circ$. In short, our results imply that for the whole AGN to be viable sources of UHECR, either appreciable amount of additional isotropic background or the large smearing effect is required. This situation for AGN as UHECR sources can be improved by narrowing down the UHECR sources from the whole AGN to a certain subclass of AGN. We tried the distance binning as an illustration and found that the AGN residing in the distance range $60 - 80$ Mpc have a good correlation with the updated PAO data. This good

correlation may be a happening by chance, but may also be an indication that the large scale structures surrounding AGN can be important for the production of UHECR. In this regard, the research on the possibility that the subclass of AGN is responsible for UHECR is very interesting and is in progress.

ACKNOWLEDGMENT

This research was supported by Basic Science Research Program through the National Research Foundation (NRF) funded by the Ministry of Education, Science and Technology (2011-0002617).

[1] J. Abraham *et al.* [Pierre Auger Collaboration], “Observation of the suppression of the flux of cosmic rays above 4×10^{19} eV,” *Phys. Rev. Lett.* **101**, 061101 (2008) [arXiv:0806.4302 [astro-ph]].

[2] R. U. Abbasi *et al.* [HiRes Collaboration], “Observation of the GZK cutoff by the HiRes experiment,” *Phys. Rev. Lett.* **100**, 101101 (2008) [arXiv:astro-ph/0703099].

[3] T. Kashti and E. Waxman, “Searching for a Correlation Between Cosmic-Ray Sources Above 10^{19} eV and Large-Scale Structure,” *JCAP* **0805**, 006 (2008) [arXiv:0801.4516 [astro-ph]].

[4] H. B. J. Koers and P. Tinyakov, “Testing large-scale (an)isotropy of ultra-high energy cosmic rays,” *JCAP* **0904**, 003 (2009). [arXiv:0812.0860 [astro-ph]].

[5] H. Takami, T. Nishimichi, K. Yahata and K. Sato, “Cross-Correlation between UHECR Arrival Distribution and Large-Scale Structure,” *JCAP* **0906**, 031 (2009) [arXiv:0812.0424 [astro-ph]].

[6] H. Takami, T. Nishimichi and K. Sato, “Systematic Survey of the Correlation between Northern HECR Events and SDSS Galaxies,” arXiv:0910.2765 [astro-ph.HE].

[7] A. J. Cuesta and F. Prada, “The correlation of UHECR with nearby galaxies in the Local Volume,” arXiv:0910.2702 [astro-ph.HE].

[8] J. Abraham *et al.* [Pierre Auger Collaboration], “Correlation of the highest energy cosmic rays with nearby extragalactic objects,” *Science* **318**, 938 (2007) [arXiv:0711.2256 [astro-ph]].

[9] J. Abraham *et al.* [Pierre Auger Collaboration], “Correlation of the highest-energy cosmic rays with the positions of nearby active galactic nuclei,” *Astropart. Phys.* **29**, 188 (2008) [Erratum-*ibid.* **30**, 45 (2008)] [arXiv:0712.2843 [astro-ph]].

[10] P. Abreu *et al.* [Pierre Auger Observatory Collaboration], “Update on the correlation of the highest energy cosmic rays with nearby extragalactic matter,” arXiv:1009.1855 [Unknown].

[11] R. U. Abbasi *et al.*, “Search for Correlations between HiRes Stereo Events and Active Galactic Nuclei,” *Astropart. Phys.* **30**, 175 (2008) [arXiv:0804.0382 [astro-ph]].

[12] R. U. Abbasi *et al.* [HiRes Collaboration], “Search for Cross-Correlations of Ultra-High-Energy Cosmic Rays with BL Lacertae Objects,” *Astrophys. J.* **636**, 680 (2006) [arXiv:astro-ph/0507120].

[13] D. S. Gorbunov, P. G. Tinyakov, I. I. Tkachev and S. V. Troitsky, “Testing the correlations between ultra-high-energy cosmic rays and BL Lac type objects with HiRes stereoscopic data,” *JETP Lett.* **80**, 145 (2004) [*Pisma Zh. Eksp. Teor. Fiz.* **80**, 167 (2004)] [arXiv:astro-ph/0406654].

- [14] S. Singh, C. P. Ma and J. Arons, “Gamma-Ray Bursts and Magnetars as Possible Sources of Ultra High Energy Cosmic Rays: Correlation of Cosmic Ray Event Positions with IRAS Galaxies,” *Phys. Rev. D* **69**, 063003 (2004) [arXiv:astro-ph/0308257].
- [15] A. Smiakowski, M. Giller and W. Michalak, “Luminous infrared galaxies as possible sources of the UHE cosmic rays,” *J. Phys. G* **28**, 1359 (2002) [arXiv:astro-ph/0203337].
- [16] D. F. Torres, E. Boldt, T. Hamilton and M. Loewenstein, “Nearby quasar remnants and ultra-high energy cosmic rays,” *Phys. Rev. D* **66**, 023001 (2002) [arXiv:astro-ph/0204419].
- [17] H. B. Kim and J. Kim, “Statistical Analysis of the Correlation between Active Galactic Nuclei and Ultra-High Energy Cosmic Rays,” *JCAP* **1103**, 006 (2011) [arXiv:1009.2284 [astro-ph.HE]].
- [18] M. P. Veron-Cetty and P. Veron, *Astron. Astrophys.* **518**, A10 (2010).
- [19] P. Sommers, “Cosmic Ray Anisotropy Analysis with a Full-Sky Observatory,” *Astropart. Phys.* **14**, 271 (2001) [arXiv:astro-ph/0004016].
- [20] M. A. Stephens, “Use of the Kolmogorov-Smirnov, Crammer-Von Mises and Related Statistics Without Extensive Tables,” *J. Royal Stat. Soc. B* **32**, 115 (1970).
- [21] D. Gorbunov, P. Tinyakov, I. Tkachev and S. V. Troitsky, “Comment on ‘Correlation of the Highest-Energy Cosmic Rays with Nearby Extragalactic Objects’,” *JETP Lett.* **87**, 461 (2008) [arXiv:0711.4060 [astro-ph]].
- [22] D. Harari, S. Mollerach and E. Roulet, “Kolmogorov-Smirnov test as a tool to study the distribution of ultra-high energy cosmic ray sources,” *Mon. Not. Roy. Astron. Soc.* **394**, 916 (2009) [arXiv:0811.0008].
- [23] A. A. Abdo and f. L. Collaboration, “The First Catalog of Active Galactic Nuclei Detected by the Fermi Large Area Telescope,” *Astrophys. J.* **715**, 429 (2010) [arXiv:1002.0150 [astro-ph.HE]].
- [24] M. R. George, A. C. Fabian, W. H. Baumgartner, R. F. Mushotzky and J. Tueller, “On Active Galactic Nuclei as Sources of Ultra-High Energy Cosmic Rays,” *Mon. Not. Roy. Astron. Soc.* **388**, L59 (2008) [arXiv:0805.2053].
- [25] J. Tueller, W. H. Baumgartner, C. B. Markwardt, G. K. Skinner, R. F. Mushotzky, M. Ajello, S. Barthelmy and A. Beardmore *et al.*, *Astrophys. J. Suppl.* **186**, 378 (2010) [arXiv:0903.3037 [astro-ph.HE]].
- [26] R. S. Nemmen, C. Bonatto and T. Storchi-Bergmann, “A correlation between the highest energy cosmic rays and nearby active galactic nuclei detected by Fermi,” *Astrophys. J.* **722**, 281 (2010) [arXiv:1007.5317 [astro-ph.HE]].
- [27] Y. Y. Jiang, L. G. Hou, X. H. Sun, W. Wang and J. L. Han, “Do Ultrahigh Energy Cosmic Rays Come from Active Galactic Nuclei and Fermi γ -ray Sources?,” *Astrophys. J.* **719**, 459 (2010) [arXiv:1004.1877 [astro-ph.HE]].
- [28] C. D. Dermer and S. Razzaque, “Acceleration of Ultra-High Energy Cosmic Rays in the Colliding Shells of Blazars and GRBs: Constraints from the Fermi Gamma ray Space Telescope,” *Astrophys. J.* **724**, 1366 (2010) [arXiv:1004.4249 [astro-ph.HE]].
- [29] D. Ryu, S. Das and H. Kang, “Intergalactic Magnetic Field and Arrival Direction of Ultra-High-Energy Protons,” *Astrophys. J.* **710**, 1422 (2010) [arXiv:0910.3361 [astro-ph.HE]].